MicroRNA-381 reduces inflammation and infiltration of macrophages in polymyositis via downregulating HMGB1

YUTAO LIU*, YUAN GAO*, JING YANG, CHANGHE SHI, YANLIN WANG and YUMING XU

Department of Neurology, The First Affiliated Hospital of Zhengzhou University, Zhengzhou, Henan 450052, P.R. China

Received February 8, 2018; Accepted May 24, 2018

DOI: 10.3892/ijo.2018.4463

Abstract. The downregulation of microRNA (miR)-381 has been detected in various diseases. The present study aimed to investigate the effects, and underlying mechanisms of miR-381 on inflammation and macrophage infiltration in polymyositis (PM). A mouse model of experimental autoimmune myositis (EAM) was generated in this study. Hematoxylin and eosin staining was conducted to detect the inflammation of muscle tissues. In addition, ELISA and immunohistochemistry were performed to determine the expression levels of associated factors, and reverse transcription-quantitative polymerase chain reaction and western blotting were used to detect the expression levels of related mRNAs and proteins. A luciferase activity assay was used to confirm the binding of miR-381 and high mobility group box 1 (HMGB1) 3' untranslated region. Transwell assays were also performed to assess the migratory ability of macrophages. The results demonstrated that serum creatine kinase (s-CK), HMGB1 and cluster of differentiation (CD)163 expression in patients with PM were increased compared within healthy controls. Conversely, the expression levels of miR-381 were downregulated in patients with PM. Furthermore, high HMGB1 expression was associated with poor survival rate in patients with PM. In the mouse studies, muscle inflammation and CD163 expression were decreased in the anti-IL-17 and anti-HMGB1 groups, compared with in the EAM model group. The expression levels of s-CK, HMGB1, IL-17 and intercellular adhesion molecule (ICAM)-1 were also downregulated in response to anti-IL-17 and anti-HMGB1. These findings indicated that HMGB1 was closely associated with inflammatory responses. In addition, the present study indicated that transfection of macrophages with miR-381 mimics reduced the migration of inflammatory macrophages, and the expression levels of HMGB1, IL-17 and ICAM-1. Conversely, miR-381 inhibition exerted the opposite effects. The effects of miR-381 inhibitors were reversed by HMGB1 small interfering RNA. In conclusion, miR-381 may reduce inflammation and the infiltration of macrophages; these effects were closely associated with the downregulation of HMGB1.

Correspondence to: Dr Yuming Xu, Department of Neurology, The First Affiliated Hospital of Zhengzhou University, 1 East Jianshe Road, Zhengzhou, Henan 450052, P.R. China
E-mail: xuyuming@zzu.edu.cn

*Contributed equally

Key words: miR-381, HMGB1, macrophage, inflammatory, IL-17, ICAM-1, polymyositis

Introduction

Polymyositis (PM) is a systemic autoimmune disease, which is characterized by progressive muscular atrophy as a result of chronic muscular inflammation (1). PM has been reported to be associated with a high risk of carcinogenesis (2,3); however, the exact mechanisms underlying the etiology and pathology of PM remain to be fully understood. The combined action of natural immunity, acquired immunity and nonimmune processes may lead to skeletal muscle injury in patients with PM (4). Various immune cells, cytokines and chemokines, as well as endoplasmic reticulum stress and autophagy participate in the pathogenesis of PM (5-9). Identifying the pathogenesis and key immune regulatory pathway of PM may improve understanding of the progression of PM, and may result in the identification of potential diagnostic and drug treatment targets that enable the future targeting of PM and PM-associated cancers.

High-mobility group box 1 (HMGB1) is a conserved non-histone nuclear protein that is widely identified in the lymph, brain, liver, lung, heart, kidney and other tissues. HMGB1 controls the stability of nucleosomes, DNA recombination, replication, repair and transcription in nucleus (10). HMGB1 is secreted to the extracellular environment where it induces cytokine production, and is involved in the pathological processes of sepsis, cancer and arthritis (11,12). HMGB1 may also be released by cellular necrosis, and it functions critically in natural and acquired immunity (13-15). It has previously been reported that activation of HMGB1 is closely associated with the development of PM (16). Therefore, the present study aimed to investigate whether HMGB1 is a potential therapeutic target for PM.

Cluster of differentiation (CD)163, which is a member of the class B scavenger receptor-cysteine-rich family, is exclusively expressed in the monocyte-macrophage system. The positive expression of CD163 has been detected in inflamed tissues, and CD163 serves an important role in the anti-inflammatory response (17). IL-17 is a proinflammatory cytokine released by T-helper cells, which induces the expression of IL-1β, IL-6, TNF-α and granulocyte-colony stimulating

factor (G-CSF) (18). Numerous studies have focused on IL-17, most of which concern common autoimmune diseases, including rheumatoid arthritis (19,20), systemic lupus erythematosus (21,22), multiple sclerosis (23,24) and atherosclerosis (25,26). Intercellular adhesion molecule (ICAM)-1 is expressed on the surface of numerous classes of cells, including endothelial cells and immune cells. In addition, ICAM-1 is induced by cell factors, including IL-1, TNF-α and bacterial lipopolysacharide (27). A previous study confirmed that the synergistic effects of IL-17 and TNF-α enhance ICAM-1 expression in several inflammatory diseases (28).

MicroRNAs (miRNAs/miRs) are a class of non-coding, single-stranded small RNA molecules, which regulate the expression of target genes (29). miRNAs possess numerous biological functions in cellular development, multiplication, variation and apoptosis (30-33). The dysregulation of miR-381 has been detected in various diseases, including acquired immunodeficiency syndrome (34), gastric cancer (35) and chondropathy (36). Therefore, it was hypothesized that miR-381 may play an important role in PM. The present study aimed to explore the role of miR-381 in PM and to investigate the mechanism underlying the effects of miR-381 on inflammation and macrophage infiltration.

Materials and methods

Ethics statement. The present study was approved by the ethics committee of the First Affiliated Hospital of Zhengzhou University (Zhengzhou, China).

Clinical samples. A total of 25 patients with PM (male:female, 12:13; age range, 40-80 years; average age, 60 years) were recruited from the First Affiliated Hospital of Zhengzhou University between June 2014 and May 2016. All enrolled patients were treated with high-dose dexamethasone, and individual patients were treated with tacrolimus or mercaptopurine. Muscle tissue samples were obtained from each patient: One sample was obtained prior to treatment and the other was obtained after treatment. Four men and six women were included in the healthy control group; these individuals had no clinical signs of muscle disease (mean age, 60 years). The clinical features of the selected patients and healthy control individuals are listed in Table I.

Sample collection. Serum samples were collected from the 25 patients with PM pretreatment and post-treatment. Serum samples were also collected from the healthy controls. Briefly, the blood samples were collected into anticoagulant tubes and centrifuged at 1,000 x g for 10 min at 4˚C. The serum samples were then maintained at -80˚C for subsequent analyses. Written informed consent was obtained from the participants.

Animal model. A mouse model of experimental autoimmune myositis (EAM) was generated in the present study. BALB/c mice were obtained from Guangdong Medical Laboratory Animal Center (Foshan, China). The mice were housed under the following conditions: Temperature, 21˚C; humidity, 40-60%; 12-h light/dark cycle and free access to food and water. Briefly, 1.5 mg rabbit myosin (M1636) and an equal volume of complete Freund's adjuvant (CFA, 1 mg/ml, F5881) (both from Sigma-Aldrich; Merck KGaA, Darmstadt, Germany) were mixed, after which 1 ml CFA mixed with 5 mg Mycobacterium tuberculosis (cat. no. 231141; BD Biosciences, Franklin Lakes, NY, USA) was added to the mixture. The obtained reagent was initially injected into the left hind leg of mice. After 1 week, it was injected into the tail root of mice. Furthermore, all of the mice were intraperitoneally injected with pertussis toxin (PT, cat. no. P2980; Sigma-Aldrich; Merck KGaA; 200 μl normal saline mixed with 500 ng PT) alongside each of the two previous injections. Healthy adult female BALB/c mice (weight, 15-18 g; age, 5-6 weeks) were randomly divided into the following groups (n=5 mice/group): Control group, in which mice were untreated; model group, in which mice underwent EAM induction; anti-IL-17 group, in which EAM mice were injected daily with anti-IL-17 antibody (100 μg/mice, cat. no. 13838; Cell Signaling Technology, Inc., Danvers, MA, USA) 14 days post-EAM induction; and anti-HMGB1 group, in which EAM mice were intraperitoneally injected with anti-HMGB1 antibody daily (100 μg/mice, cat. no. 6893; Cell Signaling Technology, Inc.) 14 days post-EAM induction. All animals were euthanized by rapid cervical dislocation 4 weeks after antibody injection. The animal study was approved by the Ethics Committee of the First Affiliated Hospital of Zhengzhou University.

Hematoxylin and eosin staining assay. The mouse muscle tissues were fixed with 4% paraformaldehyde for 6 h at room temperature. After dehydration with ethanol (from a low concentration to a high concentration), the tissues were embedded in paraffin. Paraffin-embedded mouse muscle tissues were then sliced into 4-6 μm sections and the sections were mounted onto the slides. The slides were placed into hematoxylin (Beijing Solarbio Science & Technology Co., Ltd., Beijing, China) for 10 min at room temperature. After being washed with tap water for 1-2 min, the slides were then placed in 10% glacial acetic acid for 10 sec and placed in 1% ammonia water until the sections turned blue. Subsequently, after being washed with tap water for 1-2 min, the slides were placed in eosin (Beijing Solarbio Science & Technology Co., Ltd.) for 10 sec. After dehydration in a gradual series of ethanol (70, 90, 95 and 100%), the slides were placed in xylene for 2 min; this step was repeated once. Finally, the slides were sealed with neutral gum. The slides were observed under an inverted microscope, in order to count the percentage of inflammatory cells in the whole field. The histopathologic scores were evaluated as follows: 0 score, no inflammatory cells; 1 score, <25% inflammatory cells; 2 score, 25-50% inflammatory cells; 3 score, >75% inflammatory cells.

Immunohistochemistry. Muscle tissues obtained from the patients or mice, were fixed in 4% paraformaldehyde and 30% sucrose solution at 4˚C for 73 h. The tissue samples were embedded in paraffin and then dissected into sections (4-6 μm). Following treatment with 3% hydrogen peroxide in methanol for 30 min at room temperature, the slides were incubated with primary antibodies against CD163 (1:500 dilution, cat. no. ab182422; Abcam, Cambridge, MA, USA) at 4˚C overnight. The tissue samples were then incubated with horseradish peroxidase-conjugated goat anti-rabbit immunoglobulin G (IgG) secondary antibodies (1:1,000 dilution,

Table I. Clinical data of patients with PM and healthy controls.

No.	Age (years)	Sex	Diagnosis	Duration (months)	Treatment
1	45	F	PM	8	DXMS, TAC
2	69	F	PM	4	DXMS
3	55	M	PM	9	DXMS
4	78	F	PM	5	DXMS, TAC
5	56	F	PM	14	DXMS
6	63	M	PM	3	DXMS
7	52	F	PM	5	DXMS
8	59	M	PM	13	DXMS, MER
9	48	M	PM	18	DXMS, TAC
10	61	M	PM	6	DXMS
11	75	F	PM	11	DXMS, MER
12	54	M	PM	4	DXMS
13	55	F	PM	8	DXMS
14	68	F	PM	10	DXMS
15	43	M	PM	7	DXMS
16	49	F	PM	8	DXMS, MER
17	57	M	PM	3	DXMS
18	62	F	PM	3	DXMS
19	64	F	PM	5	DXMS, TAC
20	58	M	PM	12	DXMS, MER
21	73	M	PM	14	DXMS
22	79	M	PM	8	DXMS, MER
23	54	F	PM	3	DXMS
24	62	M	PM	6	DXMS
25	74	F	PM	8	DXMS, TAC
26	52	F	-	-	-
27	64	F	-	-	-
28	62	M	-	-	-
29	76	M	-	-	-
30	54	F	-	-	-
31	80	M	-	-	-
32	46	M	-	-	-
33	55	F	-	-	-
34	48	F	-	-	-
35	79	F	-	-	-

DXMS, dexamethasone; F, female; M, male; MER, mercaptopurine; PM, polymyositis; TAC, tacrolimus.

Table II. Primer sequences used in the reverse transcription-quantitative polymerase chain reaction analysis.

Gene	Sequence (5'-3')
HMGB1	F: AAGAAGTGCTCAGAGAGGTGGAAG
	R: CTAGTTTCTTCGCAACATCACCA
IL-17	F: TACCTCAACCGTTCCACTTCACCC
	R: GGCACTTCTCAGGCTCCCTCTTC
ICAM-1	F: GGAGACTAACTGGATGAAAGACGA
	R: TCCCACGGAGCAGCACTACT
GAPDH	F: TGTCATATTTCTCGTGGTTCA
	R: TGTCATATTTCTCGTGGTTCA
miR-381	F: AAAGCGAGGTTGCCCTTTGT
	R: TACTCACAGAGAGCTTGCCC
U6	F: CTCGCTTCGGCAGCACA
	R: AACGCTTCACGAATTTGCGT
s-CK	F: CTCACCCCCACCATCTATGC
	R: GATGCATCCAGGTCCGTAGG

F, forward; HMGB1, high mobility group box protein 1; ICAM-1, intercellular adhesion molecule 1; IL-17, interleukin-17; miR-381, microRNA-381; R, reverse; s-CK, serum-creatine kinase.

cat. no. ab6721; Abcam) at room temperature for 2 h. Finally, the tissue samples were treated with DAB (Sigma-Aldrich; Merck KGaA). Cells in the negative group were incubated with nonspecific IgG (1:500 dilution, cat. no. ab108337; Abcam).

Isolation of peritoneal macrophages. As previously described (37), isolation of peritoneal macrophages was conducted. Briefly, the normal mice were euthanatized by rapid cervical dislocation and were disinfected in 70% ethanol for 5 min. Under sterile conditions, a small incision was made along the midline of the mice with sterile scissors. Subsequently, pre-chilled saline (4˚C) was injected into the peritoneal cavity; fluid from the peritoneum was aspirated and was transferred into a 50-ml conical polypropylene centrifuge tube on ice. The peritoneal exudate cells were centrifuged at 400 x g for 10 min at 4˚C. Following removal of the supernatant, the cells were resuspended in cold Dulbecco's modified Eagle's medium (DMEM; Gibco; Thermo Fisher Scientific, Inc., Waltham, MA, USA) and were gently pipetted up and down. The cells were then seeded at a density of $1x10^6$/ml in RPMI-1640 medium (Thermo Fisher Scientific, Inc.) and incubated at 37˚C in an incubator containing 5% CO_2. Following 2 h incubation, the macrophages were grouped as follows: Control group, which consisted of untreated cells; negative control (NC)-mimics group, in which cells were transfected with NC mimics; mimics group, in which cells were transfected with miR-381 mimics; NC-inhibitors group, in which cells were transfected with NC inhibitors negative control; inhibitors group, in which cells were transfected with miR-381 inhibitors; NC-small interfering (si)RNA, in which cells were transfected with NC siRNA (no specific sequence); and inhibitors + siRNA-HMGB1group, in which cells were co-transfected with miR-381 inhibitors and siRNA-HMGB1.

Cell transfection. The cells were seeded into a 6-well plate at a density of $3x10^4$/well. Once cell confluence reached 70%, the cells were transfected with miRNA (50 nM) and/or siRNA (50 pmol) using Lipofectamine® 3000 (Invitrogen; Thermo Fisher Scientific, Inc.) at 37˚C. After 48 h, the cells underwent further experimentation. The miRNAs and siRNA used were as follows: miR-381 mimics (miR10017081-1-5); miRNA negative control (miR01201-1-5); miR-381 inhibitor (miR20017081-1-5); miRNA inhibitor control (miR02201-1-5) (all from Guangzhou RiboBio Co., Ltd., Guangzhou, China); si-HMGB1 (MBS8222378) and siRNA negative control (NC) (MBS8241404) (both from MyBioSource, San Diego, CA, USA).

ELISA. The secreted levels of IL-17 (mouse, M1700; human, D1700) and ICAM-1 (mouse, MIC100; human, Dy720) were detected using ELISA kits (R&D Systems, Inc., Minneapolis, MN, USA). The mouse serum creatine kinase (s-CK) ELISA kit (CSB-E14407m) was purchased from Cusabio Technology LLC (Houston, TX, USA). The human s-CK ELISA kit (NR-R10105) and the HMGB1 ELISA kits (mouse, NB-S11134; human BG-HUM11133) were purchased from Novatein Biosciences, Inc., (Woburn, MA, USA). All experiments were performed according to the manufacturer's protocols. Finally, the optical density at 450 nm was measured on a microplate reader (Bio-Rad Laboratories, Inc., Hercules, CA, USA).

Reverse transcription-quantitative polymerase chain reaction (RT-qPCR) analysis. The mouse tissues were ground in liquid nitrogen; total RNA from tissues and cultured cells was extracted by TRIzol® (Invitrogen; Thermo Fisher Scientific, Inc.). Subsequently, 2 μg RNA was used for cDNA synthesis using first strand cDNA kit (Sigma-Aldrich; Merck KGaA), according to the manufacturer's protocol. RT-qPCR was performed using the SYBR Green Premix Reagent (Takara Bio, Inc., Otsu, Japan) on an ABI 7500 Thermocycler (Applied Biosystems; Thermo Fisher Scientific, Inc.). The qPCR thermocycling conditions were as follows: 94˚C for 5 min; followed by 30 cycles at 94˚C for 30 sec and 60˚C for 30 sec; and a final extension step at 72˚C for 10 min. GAPDH/U6 was used as an internal control. The sequences of the primers (Invitrogen; Thermo Fisher Scientific, Inc.) used for PCR amplification are indicated in Table II.

Western blotting. The collected tissues were ground in liquid nitrogen and proteins were isolated using the total extraction sample kit (Sigma-Aldrich; Merck KGaA). Cultured cells were lysed on ice in radioimmunoprecipitation assay lysis buffer (pH 7.4; 1 mM $MgCl_2$, 1% Triton X-100, 10 mM Tris-HCl and 0.1% SDS). Protein concentration was determined using the bicinchoninic acid protein assay kit (Bio-Rad Laboratories, Inc.). An equal quantity (50 μg) of protein from each sample was separated by 8% SDS-PAGE and transferred onto nitrocellulose membranes (EMD Millipore, Billerica, MA, USA). Nonspecific antigens were blocked by immersing the membranes in 5% non-fat milk at room temperature for 2 h. Subsequently, the membranes were incubated overnight at 4˚C with the following primary antibodies: Anti-HMGB1 (1:500 dilution, cat. no. ab18256), anti-IL-17 (1:5,000 dilution, cat. no. ab9565), anti-ICAM-1 (1:1,000 dilution, cat. no. ab2213) and anti-GAPDH (1:2,500 dilution, cat. no. ab9485) (all from Abcam). The membranes were then incubated with the corresponding horseradish peroxidase-conjugated secondary antibodies (1:2,000; cat. nos. ab6789 and ab6721; Abcam) at room temperature for 1 h. The signals were detected using an enhanced chemiluminescence reagent (EMD Millipore). The blots were analyzed using Quantity One software version 4.62 (Bio-Rad Laboratories).

Luciferase activity assay. Bioinformatics prediction was performed using the online databases TargetScan (http://www.targetscan.org/) and miRDB (http://www.mirdb.org/). The HMGB1-3' untranslated region (3'UTR) was synthesized by Invitrogen; Thermo Fisher Scientific, Inc. The HMGB-3'UTR was amplified to the downstream site of pGL4 luciferase vectors (Promega Corporation, Madison, WI, USA). The HMGB1-3'UTR mutant (mut) was generated using a rapid site-directed mutagenesis kit (Thermo Fisher Scientific, Inc.). Cells were seeded at $3x10^4$/well in a 24-well plate; after 24 h, the cells were transfected with 1 μg HMGB1-3'UTR (wild-type or mut)-luciferase plasmid, 50 nM miR-381 mimics/miR-NC and 150 ng *Renilla* luciferase plasmid using Lipofectamine® 3000 (Invitrogen; Thermo Fisher Scientific, Inc.). The cells were then incubated at 37˚C for 36 h. Luciferase activity was detected using a dual-luciferase reporter assay kit (Promega Corporation), according to the manufacturer's protocol. All data were normalized to *Renilla* luciferase activity. The relative luciferase activities were expressed as relative fluorescence units.

Transwell assay. Cells (~$5x10^4$ cells/ml) were serum-starved for 24 h in serum-free DMEM at 37˚C. The cells were then plated into a 24-well Transwell plate (Corning Incorporated, Corning, NY, USA). DMEM supplemented with 15% fetal bovine serum (Gibco; Thermo Fisher Scientific, Inc.) was placed into the lower chamber. After 24 h, cells that penetrated into the lower chamber were fixed with 95% ethyl alcohol and were stained with 0.1% crystal violet at room temperature for 20 min. Finally, the cells were observed under an inverted microscope and the number of migrated cells was counted.

Statistical analysis. All experimental results are presented as the means ± standard deviation and experiments were repeated at least three times. Kaplan-Meier analysis was used for survival analysis; log rank test was used to compare the differences. The receiver operating characteristic analysis was performed to distinguish the patients with high HMGB1 expression from the patients with low HMGB1 expression. GraphPad Prism 6.0 (GraphPad, Inc., La Jolla, CA, USA) was used to perform data analysis. All assays were analyzed by one-way analysis of variance followed by Turkey's test. $P<0.05$ was considered to indicate a statistically significant difference.

Results

Expression levels of s-CK, HMGB1, IL-7 and miR-381 in healthy controls and patients with PM. Compared with in the healthy control individuals, the serum concentrations of s-CK (434±70 vs. 97±11 pg/ml), HMGB1 (348±63 vs. 102±19 pg/ml) and IL-17 (297±38 vs. 89±14 pg/ml) were markedly increased in patients with PM. However, following treatment with a glucocorticoid or other immunosuppressive drugs, s-CK (212±35 vs. 434±70 pg/ml), HMGB1 (220±38 vs. 348±63 pg/ml) and IL-17 (158±21 vs. 297±38 pg/ml) expression levels were decreased, as detected by ELISA ($P<0.05$; Fig. 1A-C). Furthermore, in patients with PM, the expression levels of HMGB1 were significantly increased, whereas the expression levels of miR-381 were markedly decreased compared with in healthy control individuals. Conversely, the expression levels of HMGB1 and miR-381 were reversed in the post-treatment group ($P<0.05$; Fig. 1D and E). As shown in Fig. 1F, patients with PM with a high expression of HMGB1 had a worse prognosis ($P=0.0204$). A receiver operating characteristic curve analysis was conducted to distinguish patients with PM

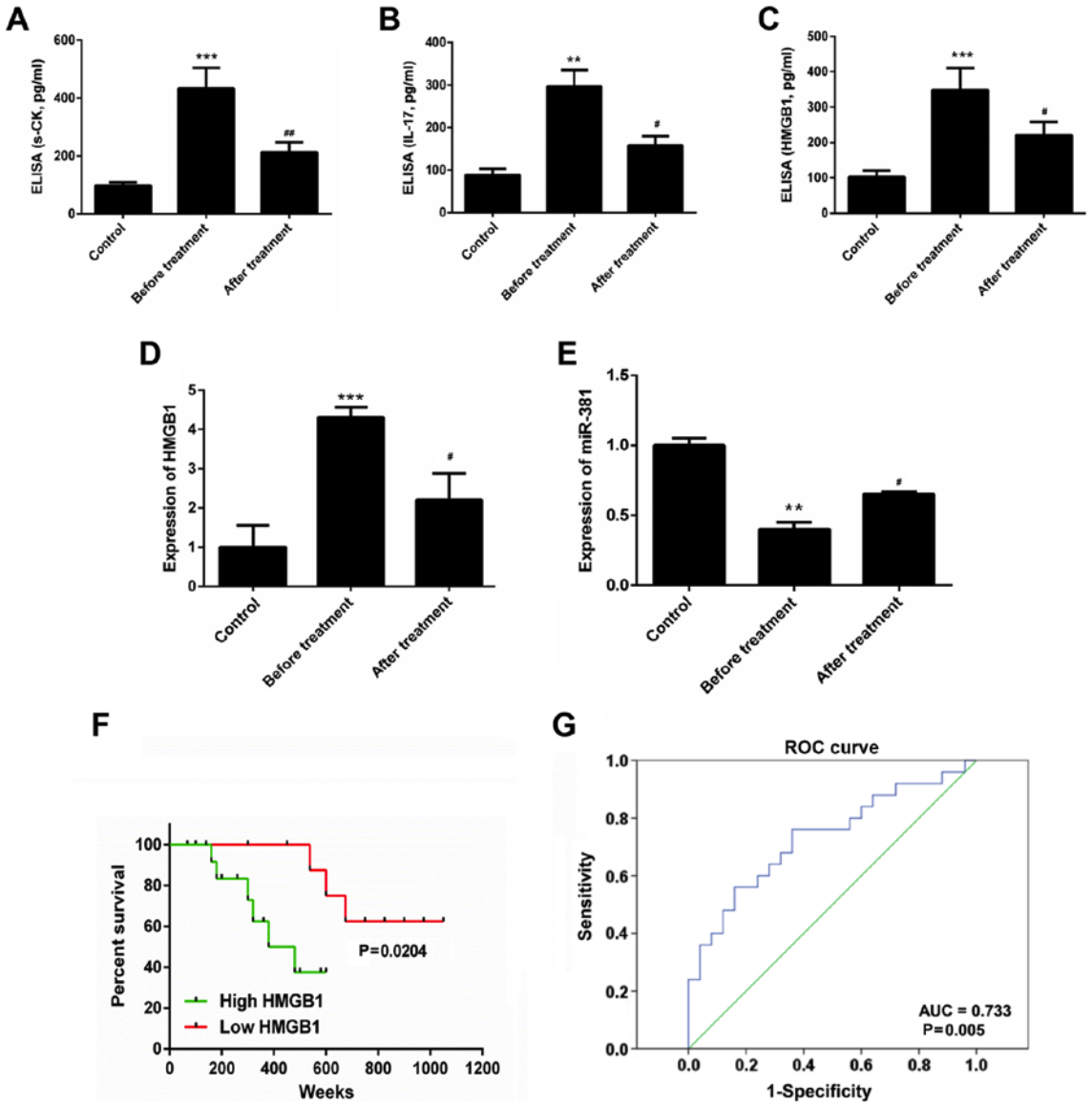

Figure 1. ELISA was performed to assess (A) s-CK, (B) IL-17 and (C) HMGB1 expression in serum samples. Reverse transcription-quantitative polymerase chain reaction analysis was conducted to detect the expression levels of (D) HMGB1 and (E) miR-381 in serum samples. (F) Overall survival rates of patients with PM based on serum HMGB1 levels, as measured by Kaplan-Meier survival analysis. P-values were calculated by the log-rank test. (G) ROC curve analysis was performed to distinguish patients with PM with high HMGB1 expression from patients with PM with low HMGB1 expression; cutoff value, 14.2 ng/ml. **P<0.01, ***P<0.01 vs. the control group. $^{\#}$P<0.05, $^{\#\#}$P<0.01 vs. the before treatment group. AUC, area under the curve; HMGB1, high mobility group box protein 1; IL-17, interleukin-17; miR-381, microRNA-381; PM, polymyositis; ROC, receiver operating characteristic.

with high HMGB1 expression from patients with PM with low HMGB1 expression. The cutoff value was 14.2 ng/ml. The area under the curve was 0.733 (Fig. 1G).

CD163 expression in muscle samples from patients with PM. Muscle samples from control, pretreatment and post-treatment groups were stained with anti-CD163. The expression of CD163 was almost negative in the control group (Fig. 2A). Conversely, strong CD163 staining was identified in the pretreatment group (Fig. 2B), whereas CD163 expression was markedly reduced in the post-treatment group (Fig. 2C).

Inflammation of muscle tissues in mice. In the mouse control group, muscle fibers were polygonal in shape and were roughly the same size. A large amount of inflammation and macrophage infiltration was detected, and muscle fibers with varied sizes were observed in the EAM model group. Conversely, inflammation and macrophage infiltration was inhibited in the anti-IL-17 and anti-HMGB1 groups, compared with in the model group (Fig. 3A). Similarly, the histopathologic score in the model group was elevated, whereas treatment with anti-IL-17 and anti-HMGB1 resulted in a reduction in histopathologic score (Fig. 3B; Table III).

Expression of CD163 in muscle samples from mice. CD163 expression was increased in the model group compared with in the control group (Fig. 4A and B). Conversely, following treatment with anti-IL-17 and anti-HMGB1, CD163 expression was markedly reduced (Fig. 4C and D).

Expression of s-CK, HMGB1, IL-7, ICAM-1 and miR-381 in mice. The results of an ELISA indicated that, compared with

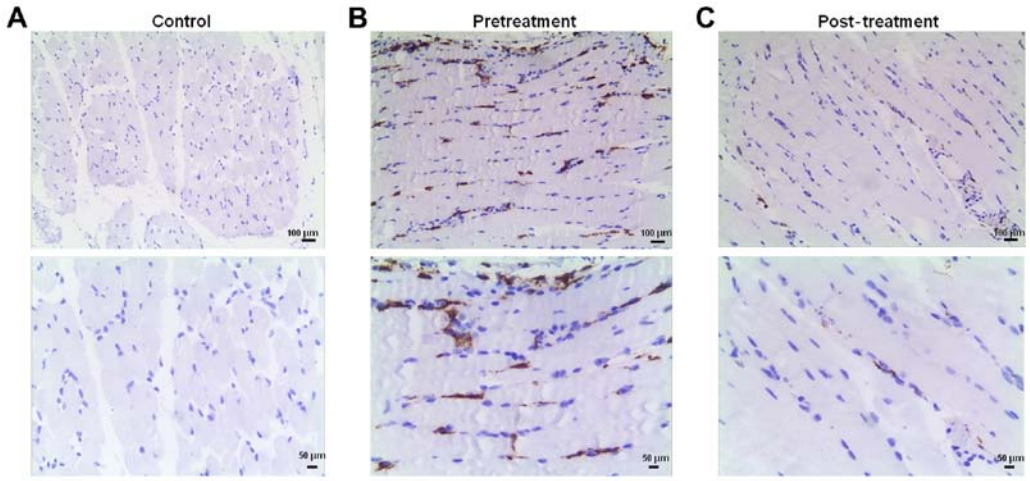

Figure 2. Immunohistochemistry was performed to evaluate cluster of differentiation 163 expression in muscle tissues from patients with polymyositis and healthy control individuals.

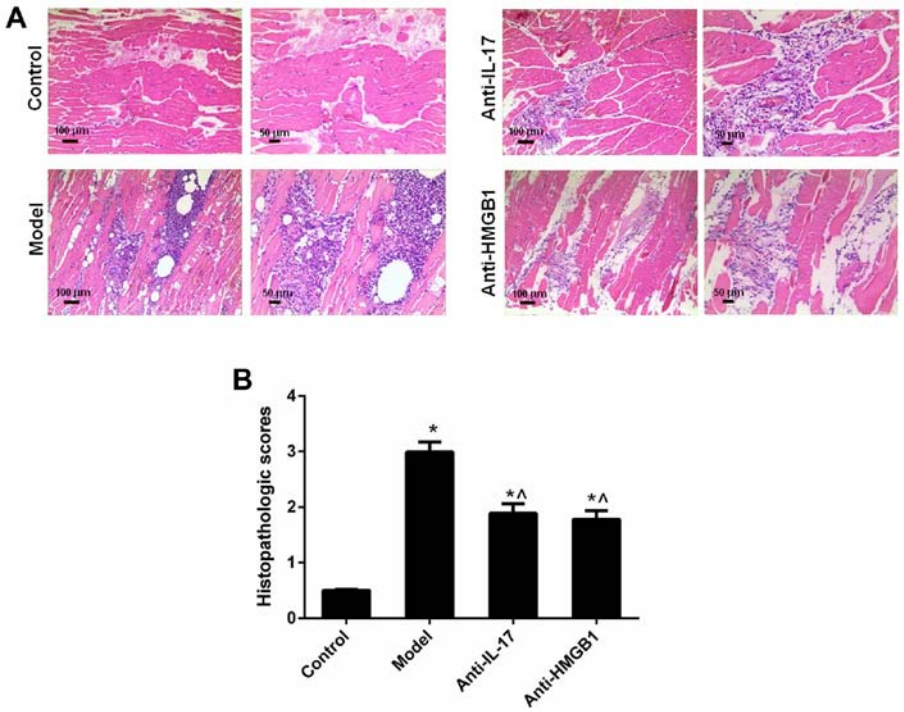

Figure 3. Hematoxylin and eosin staining assay was conducted to detect the inflammatory response of the muscle fiber. HMGB1, high mobility group box protein 1; IL-17, interleukin-17. *P<0.05 vs. the control group; ^P<0.05 vs. the model group.

Table III. Histopathologic scores of the muscle samples from the experimental autoimmune myositis model rats (n=5; mean ± standard deviation).

Group	Histopathologic scores
Control	0
Model	2.99±0.182[a]
Anti-IL-17	1.89±0.173[a,b]
Anti-HMGB1	1.78±0.156[a,b]

[a]P<0.05 vs. the control group; [b]P<0.01 vs. the model group. HMGB1, high mobility group box protein 1; IL-17, interleukin-17.

in the control group, the levels of s-CK, HMGB1 and IL-17 were significantly increased in the model group. However, the expression levels of s-CK, HMGB1 and IL-17 were reduced following anti-IL-17 and anti-HMGB1 treatment (Fig. 5A-C). Furthermore, the results of RT-qPCR and western blotting revealed that the expression levels of HMGB1, ICAM-1 and IL-17 exhibited a consistent trend with the results of the ELISA. Furthermore, the expression levels of miR-381 were reduced in the model group, whereas anti-IL-17 and anti-HMGB1 did not restore the expression of miR-381 (Fig. 5D-F).

HMGB1 may be a target gene of miR-381. Bioinformatics analysis identified a possible binding site for miR-381 in the 3'UTR of HMGB1 (Fig. 6A). The results of a luciferase assay

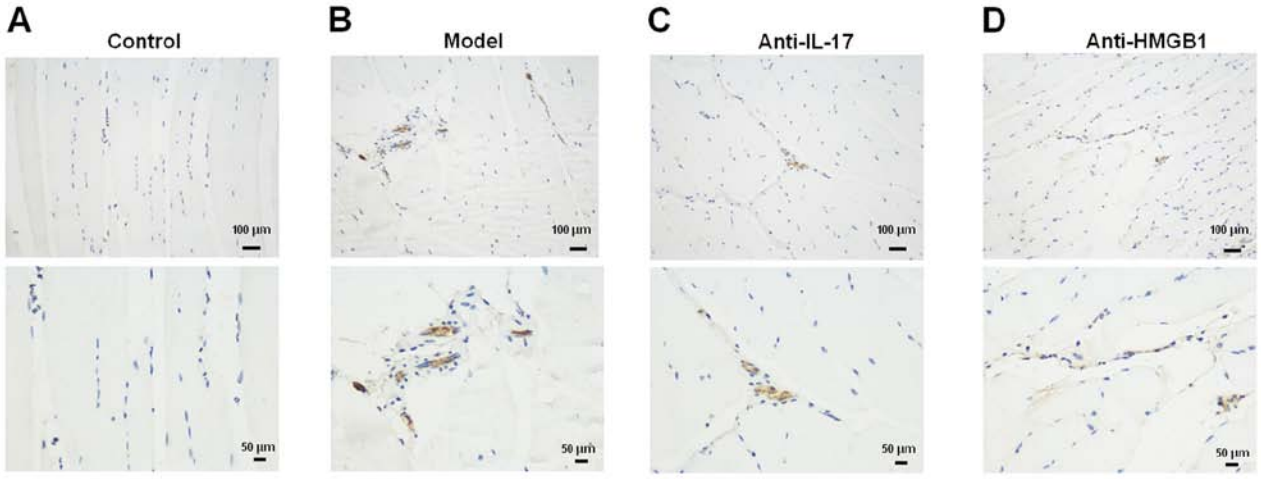

Figure 4. Immunohistochemistry was performed to assess cluster of differentiation 163 expression. HMGB1, high mobility group box protein 1; IL-17, interleukin-17.

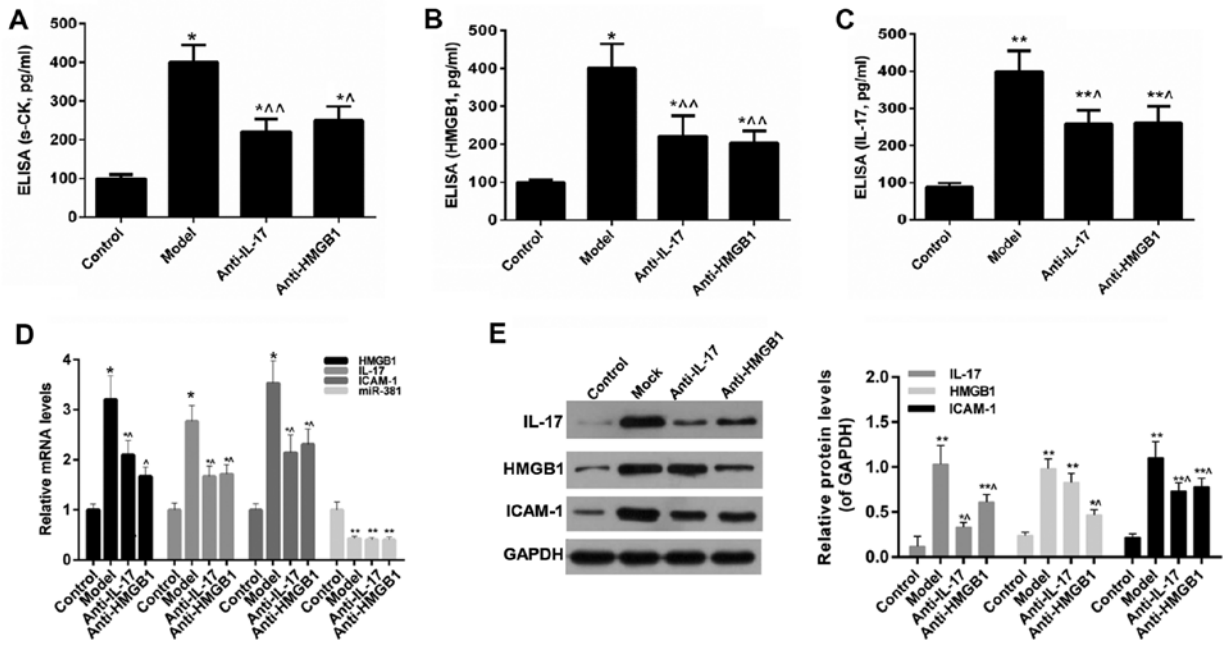

Figure 5. ELISA was performed to detect (A) s-CK, (B) HMGB1 and (C) IL-17 expression in mice. (D) Reverse transcription-quantitative polymerase chain reaction analysis was carried out to evaluate the expression levels of HMGB1, IL-17, ICAM-1 and miR-381 in mice. (E) Western blot analysis was performed to detectIL-17, HMGB1 and ICAM-1 expression in mice. *P<0.05, **P<0.01 vs. the control group; $^{\wedge}$P<0.05, $^{\wedge\wedge}$P<0.01 vs. the model group.HMGB1, high mobility group box protein 1; ICAM-1, intercellular adhesion molecule 1; IL-17, interleukin-17; miR-381, microRNA-381; s-CK, serum creatine kinase.

in cells indicated that the luciferase activity of HMGB1-3'UTR was decreased in the presence of miR-381 (Fig. 6B, P<0.05).

miR-381 reduces the migration of macrophages. As shown in Fig. 6C and D, an obvious decrease in the number of migratory cells was observed following transfection with miR-381 mimics (P<0.05). The number of migratory cells in the miR-381 inhibitors group was higher than in the other groups (P<0.05). Conversely, the effects of miR-381 inhibitors were blocked by siRNA-HMGB1.

Effects of miR-381 and HMGB1 on the expression levels of s-CK, ICAM-1 and IL-17. As shown in Fig. 7A, miR-381 expression in the miR-381 mimics group was significantly increased compared with in the other groups (P<0.05). Furthermore, an obvious decrease in miR-381 expression was observed in the miR-381 inhibitors group (P<0.05). The expression levels of HMGB1, IL-17 and ICAM-1 in macrophages were decreased following transfection with miR-381 mimics, whereas miR-381 inhibitors increased the expression levels of HMGB1, IL-17 and ICAM-1 (Fig. 7B-E). Conversely, the effects of miR-381 inhibitors were inhibited by siRNA-HMGB1.

Discussion

PM is characterized by inflammation in muscle tissues and chronic muscle weakness, and can lead to physical disability and a shortened lifespan. The necrotic muscle tissues of

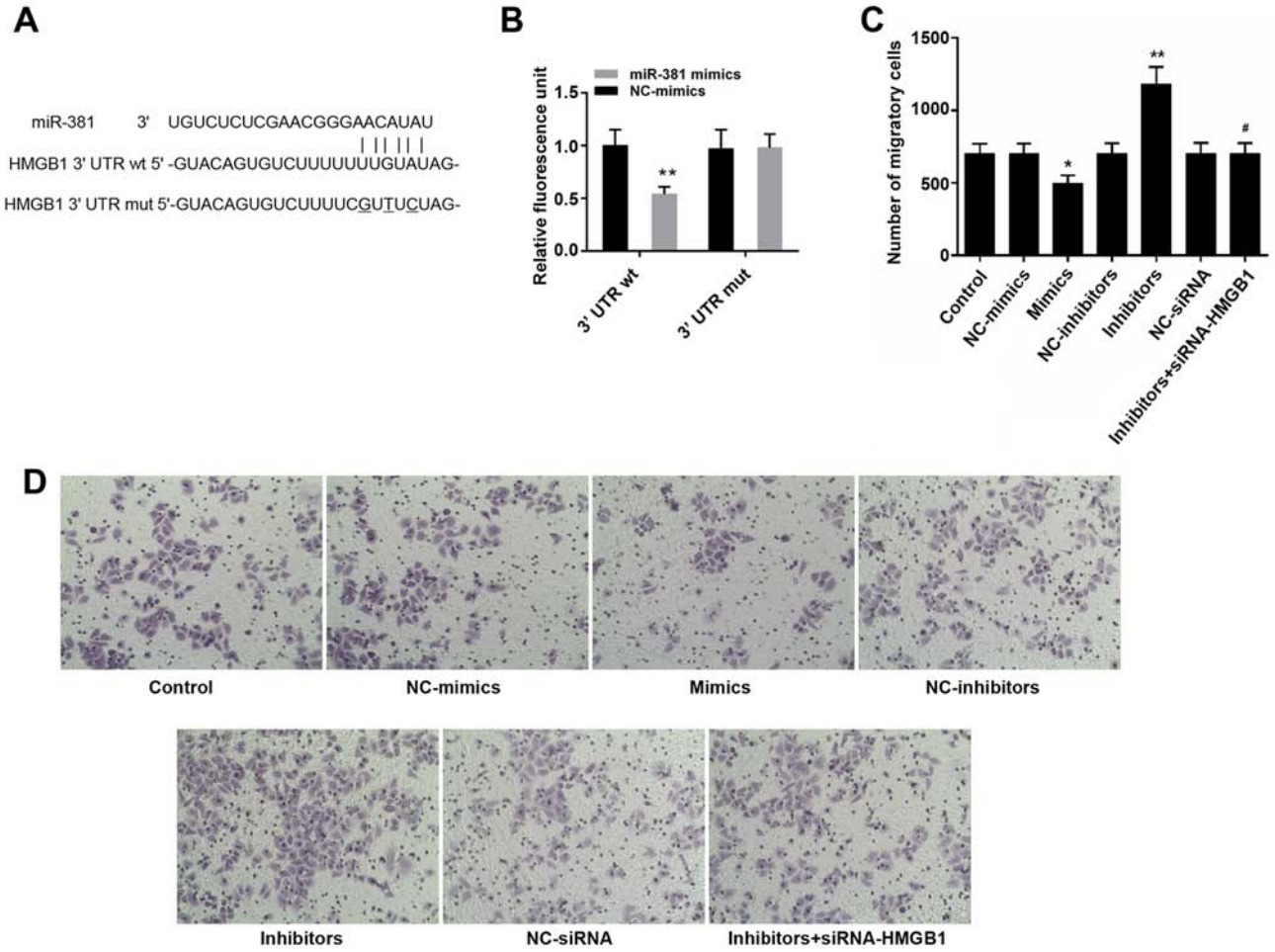

Figure 6. (A) Bioinformatics prediction of the binding between miR-381 and HMGB1-3'UTR. (B) Luciferase activity assay was conducted to assess the binding of miR-381 and HMGB1-3'UTR. (C) Number of migratory cells. (D) Images of cells that penetrated through the membrane in the control, NC-mimics, mimics, NC-inhibitors, inhibitors, NC-siRNA and inhibitors + siRNA-HMGB1 groups. Magnification, x100. *P<0.05, **P<0.01 vs. the control group; $^{\#}$P<0.05 vs. the inhibitors group. 3'UTR, 3' untranslated region; HMGB1, high mobility group box protein 1; miR-381, microRNA-381; mut, mutant; NC, negative control; siRNA, small interfering RNA; wt, wild-type.

patients with PM are mainly characterized by inflammatory cell infiltration, including the entry of macrophages into skeletal muscles (38-40). Treatment with high doses of glucocorticoids and supplementation with additional immunosuppressive drugs is a widely adopted method to treat patients with PM (41). However, the exact pathogenesis of PM is currently unclear. A recent study confirmed that cellular inflammation serves a significant role in the development of PM (42). Nevertheless, little is currently known about the explicit effects of these pathways on the progression of PM. Therefore, studies regarding the exact mechanisms underlying PM development are required.

In the present study, the expression levels of s-CK were markedly increased in patients with PM. Following treatment with high doses of glucocorticoids or immunosuppressive drugs, s-CK expression was markedly reduced. In addition, HMGB1 expression was significantly higher in patients with PM compared with in the control individuals, and a marked decrease was identified in the post-treatment group. It has previously been reported that activation of HMGB1 may be associated with the development of PM (16). Furthermore, IL-17 levels were significantly higher in patients with PM compared with in the control group, whereas IL-17 levels declined in the post-treatment group. A previous study regarding IL-17 in PM revealed that IL-17 levels are increased in PM compared with in a control group (43). The strong effects of IL-17 have been reported on the pathogenesis of numerous autoimmune diseases, including multiple sclerosis (44), rheumatoid arthritis (45) and psoriasis (46). An association between the IL-17/ ICAM-1 pathway and PM has also been reported (47-49). The present study also detected the expression levels of miR-381 in healthy controls and patients with PM. The results demonstrated that the expression levels of miR-381 were markedly reduced in the PM group compared with in the control group, whereas after treatment with drugs, miR-381 expression was distinctly higher than in the pretreatment group. The results of a survival analysis further revealed that survival time was longer in patients with PM with low HMGB1 expression. Based on these results, it may be hypothesized that HMGB1 is a critical factor in the mechanism underlying the development of PM.

The present results demonstrated that, in PM, the expression levels of HMGB1 and miR-381 exhibited opposing trends. Therefore, it was hypothesized that miR-381 might serve a critical role in the pathogenesis of PM. An EAM animal experimental model was established, in order to verify this

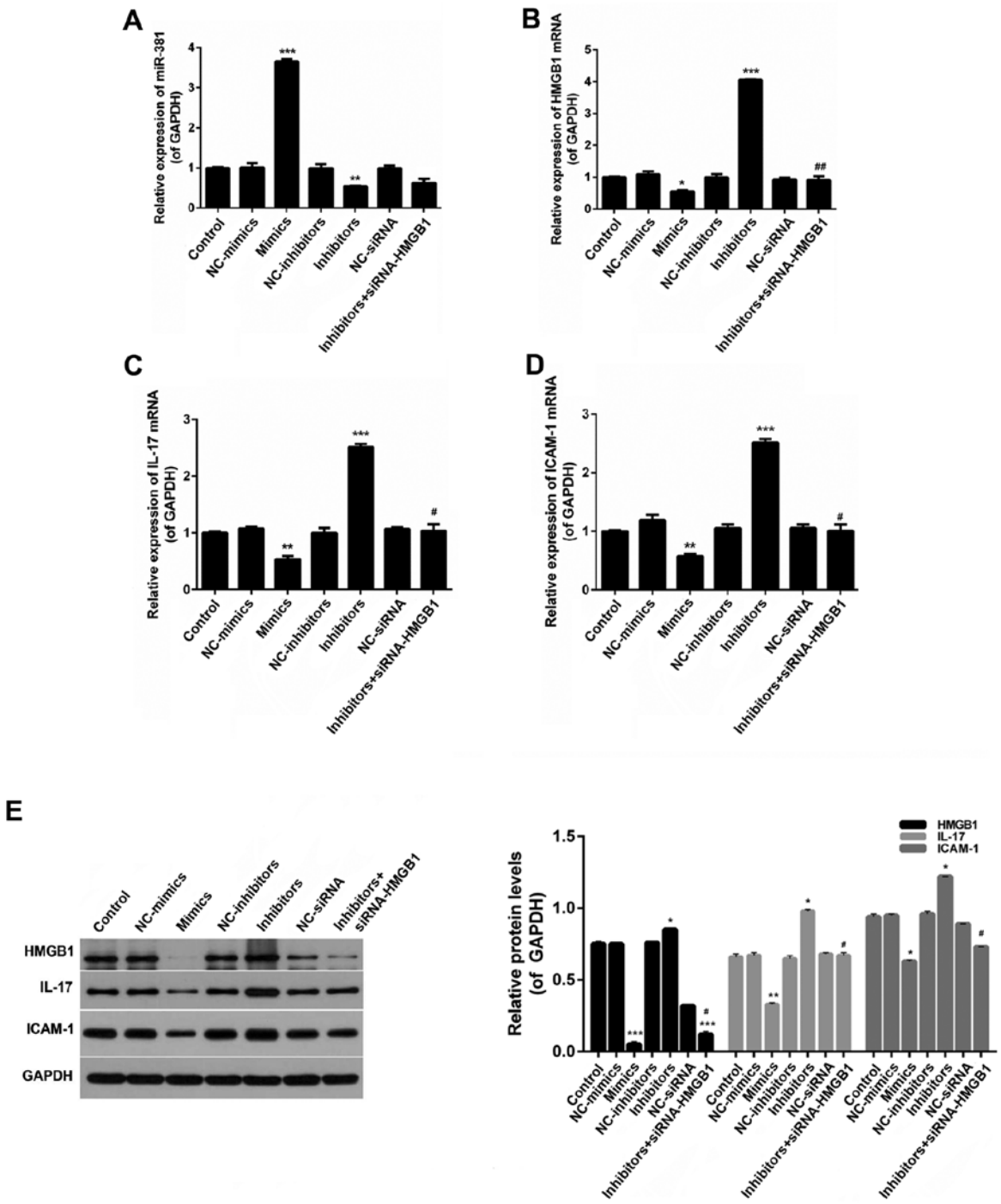

Figure 7. Reverse transcription-quantitative polymerase chain reaction analysis was performed to evaluate the expression levels of (A) miR-381, (B) HMGB1, (C) IL-17 and (D) ICAM-1 in macrophages. (E) Western blot analysis was performed to detectHMGB1, IL-17, and ICAM-1 expression in macrophages. *P<0.05, **P<0.01, ***P<0.01 vs. the control group; $^{\#}$P<0.05, $^{\#\#}$P<0.05 vs. the inhibitors group. HMGB1, high mobility group box protein 1; ICAM-1, intercellular adhesion molecule 1; IL-17, interleukin-17; miR-381, microRNA-381; NC, negative control; siRNA, small interfering RNA.

assumption. The results revealed that inflammation of muscle tissues was reduced by anti-IL-17 and anti-HMGB1, compared with in the model group. Furthermore, CD163 expression was also decreased by anti-IL-17 and anti-HMGB1. It has previously been reported that IL-17 is a proinflammatory cytokine released by T-helper cells, which may induce the expression of IL-1β, IL-6, TNF-α and G-CSF (18). Therefore, the present study confirmed that downregulation of HMGB1 may alleviate inflammatory responses. To further verify this conclusion, the expression levels of HMGB1, IL-17 and ICAM-1 were estimated. The results revealed that the increased levels of HMGB1, IL-17 and ICAM-1 could be decreased by anti-IL-17 and anti-HMGB1. This finding was consistent with the results of a previous study (50); in this previous study, it was revealed that the expression of ICAM-1 is reduced by anti-IL-17. Similarly, another study suggested that HMGB1 can stimulate the expression of IL-17 (51). These results indicated that the HMGB1-IL-17-ICAM1 pathway has a critical role in the inflammatory response of PM. Furthermore, the expression levels of miR-381 were significantly decreased

in the EAM model mice; however, treatment with anti-IL-17 and anti-HMGB1 did not increase the expression levels of miR-138, thus suggesting that miR-138 was not downstream of IL-17 or HMGB1.

To illustrate the underlying mechanism in the regulation of HMGB1, a bioinformatics analysis was conducted using available online databases. The results demonstrated that a potential binding site for miR-381 was present in the 3'UTR of HMGB1; this was confirmed by a dual luciferase assay. These findings suggested that HMGB1 may be a downstream target of miR-381; therefore, the association between HMGB1 and miR-381 was determined. The results demonstrated that transfection with miR-381 mimics inhibited the migration of macrophages, and that the expression levels of HMGB1, IL-17 and ICAM-1 were decreased. Conversely, miR-381 inhibitors exerted the opposite effects compared with miR-381 mimics, thus suggesting that miR-381 may reduce the inflammatory responses in EAM mice. Notably, transfection with si-HMGB1 suppressed the effects of miR-381 inhibitors. Taken together, these findings suggested that HMGB1 may be a downstream target of miR-381, and that miR-381 may inhibit inflammation and macrophage infiltration via downregulating the expression of HMGB1.

In conclusion, the present study indicated that miR-381 downregulated HMGB1, so as to reduce inflammation and macrophage infiltration and the expression of IL-17/ICAM-1. The present study provided a novel molecular clue to aid understanding of the progression of PM and a potential target to combat PM.

Acknowledgements

Not applicable.

Funding

The present study was supported by the National Natural Science Foundation of China to Dr Yuming Xu (grant nos. 81530037 and 81471158); the Medical Science and Technique Foundation of Henan Province to Yutao Liu (grant no. 201503038); the Key Scientific Research Projects of Universities in Henan Province to Yutao Liu (grant no. 16A320052).

Availability of data and materials

All data generated or analyzed during this study are included in this published article.

Authors' contributions

YL wrote the manuscript. YL, YG, JY and CS performed the experiments. YW and YX designed the study. YL, YG and JY performed the data analysis. YL, YG, and YX revised the manuscript and all authors reviewed the manuscript.

Ethics approval and consent to participate

The present study was approved by the ethics committee of the First Affiliated Hospital of Zhengzhou University (Zhengzhou, China). Written informed consent was obtained from the participants. The animal study was approved by the ethics committee of the First Affiliated Hospital of Zhengzhou University.

Patient consent for publication

Informed consent was obtained from all participants for the publication of their data.

Competing interests

The authors declare that they have no competing interests.

References

1. Maoz CR, Langevitz P, Livneh A, Blumstein Z, Sadeh M, Bank I, Gur H and Ehrenfeld M: High incidence of malignancies in patients with dermatomyositis and polymyositis: An 11-year analysis. Semin Arthritis Rheum 27: 319-324, 1998.
2. Wang J, Guo G, Chen G, Wu B, Lu L and Bao L: Meta-analysis of the association of dermatomyositis and polymyositis with cancer. Br J Dermatol 169: 838-847, 2013.
3. Hill CL, Zhang Y, Sigurgeirsson B, Pukkala E, Mellemkjaer L, Airio A, Evans SR and Felson DT: Frequency of specific cancer types in dermatomyositis and polymyositis: A population-based study. Lancet 357: 96-100, 2001.
4. Rayavarapu S, Coley W and Nagaraju K: An update on pathogenic mechanisms of inflammatory myopathies. Curr Opin Rheumatol 23: 579-584, 2011.
5. Fasth AE, Dastmalchi M, Rahbar A, Salomonsson S, Pandya JM, Lindroos E, Nennesmo I, Malmberg KJ, Soderberg-Naucler C, Trollmo C, *et al*: T cell infiltrates in the muscles of patients with dermatomyositis and polymyositis are dominated by CD28null T cells. Journal of immunology (Baltimore, Md : 1950) 183: 4792-4799, 2009.
6. Henriques-Pons A and Nagaraju K: Nonimmune mechanisms of muscle damage in myositis: Role of the endoplasmic reticulum stress response and autophagy in the disease pathogenesis. Curr Opin Rheumatol 21: 581-587, 2009.
7. Salajegheh M, Kong SW, Pinkus JL, Walsh RJ, Liao A, Nazareno R, Amato AA, Krastins B, Morehouse C, Higgs BW, *et al*: Interferon-stimulated gene 15 (ISG15) conjugates proteins in dermatomyositis muscle with perifascicular atrophy. Ann Neurol 67: 53-63, 2010.
8. Walsh RJ, Kong SW, Yao Y, Jallal B, Kiener PA, Pinkus JL, Beggs AH, Amato AA and Greenberg SA: Type I interferon-inducible gene expression in blood is present and reflects disease activity in dermatomyositis and polymyositis. Arthritis Rheum 56: 3784-3792, 2007.
9. Wenzel J, Scheler M, Bieber T and Tüting T: Evidence for a role of type I interferons in the pathogenesis of dermatomyositis. Br J Dermatol 153: 462-463, author reply 463-464, 2005.
10. Scovell WM: High mobility group protein 1: A collaborator in nucleosome dynamics and estrogen-responsive gene expression. World J Biol Chem 7: 206-222, 2016.
11. Musumeci D, Roviello GN and Montesarchio D: An overview on HMGB1 inhibitors as potential therapeutic agents in HMGB1-related pathologies. Pharmacol Ther 141: 347-357, 2014.
12. Yang Q, Liu X, Yao Z, Mao S, Wei Q and Chang Y: Penehyclidine hydrochloride inhibits the release of high-mobility group box 1 in lipopolysaccharide-activated RAW264.7 cells and cecal ligation and puncture-induced septic mice. J Surg Res 186: 310-317, 2014.
13. Harris HE, Andersson U and Pisetsky DS: HMGB1: A multifunctional alarmin driving autoimmune and inflammatory disease. Nat Rev Rheumatol 8: 195-202, 2012.
14. Lotze MT and Tracey KJ: High-mobility group box 1 protein (HMGB1): Nuclear weapon in the immune arsenal. Nat Rev Immunol 5: 331-342, 2005.
15. Pisetsky DS, Erlandsson-Harris H and Andersson U: High-mobility group box protein 1 (HMGB1): An alarmin mediating the pathogenesis of rheumatic disease. Arthritis Res Ther 10: 209, 2008.
16. Müller S, Scaffidi P, Degryse B, Bonaldi T, Ronfani L, Agresti A, Beltrame M and Bianchi ME: New EMBO members' review: The double life of HMGB1 chromatin protein: architectural factor and extracellular signal. EMBO J 20: 4337-4340, 2001.

17. Moestrup SK and Møller HJ: CD163: A regulated hemoglobin scavenger receptor with a role in the anti-inflammatory response. Ann Med 36: 347-354, 2004.
18. Niimoto T, Nakasa T, Ishikawa M, Okuhara A, Izumi B, Deie M, Suzuki O, Adachi N and Ochi M: MicroRNA-146a expresses in interleukin-17 producing T cells in rheumatoid arthritis patients. BMC Musculoskelet Disord 11: 209, 2010.
19. Hirota K, Hashimoto M, Yoshitomi H, Tanaka S, Nomura T, Yamaguchi T, Iwakura Y, Sakaguchi N and Sakaguchi S: T cell self-reactivity forms a cytokine milieu for spontaneous development of IL-17^{+} Th cells that cause autoimmune arthritis. J Exp Med 204: 41-47, 2007.
20. Lee YK, Mukasa R, Hatton RD and Weaver CT: Developmental plasticity of Th17 and Treg cells. Curr Opin Immunol 21: 274-280, 2009.
21. Crispin JC, Oukka M, Bayliss G, Cohen RA, Van Beek CA, Stillman IE, Kyttaris VC, Juang YT and Tsokos GC: Expanded double negative T cells in patients with systemic lupus erythematosus produce IL-17 and infiltrate the kidneys. J Immunol 181: 8761-8766, 2008.
22. Pickens SR, Volin MV, Mandelin AM, 2nd, Kolls JK, Pope RM and Shahrara S: IL-17 contributes to angiogenesis in rheumatoid arthritis. J Immunol 184: 3233-3241, 2010.
23. Langrish CL, Chen Y, Blumenschein WM, Mattson J, Basham B, Sedgwick JD, McClanahan T, Kastelein RA and Cua DJ: IL-23 drives a pathogenic T cell population that induces autoimmune inflammation. J Exp Med 201: 233-240, 2005.
24. Tzartos JS, Friese MA, Craner MJ, Palace J, Newcombe J, Esiri MM and Fugger L: Interleukin-17 production in central nervous system-infiltrating T cells and glial cells is associated with active disease in multiple sclerosis. Am J Pathol 172: 146-155, 2008.
25. Gao Q, Jiang Y, Ma T, Zhu F, Gao F, Zhang P, Guo C, Wang Q, Wang X, Ma C, *et al*: A critical function of Th17 proinflammatory cells in the development of atherosclerotic plaque in mice. J Immunol 185: 5820-5827, 2010.
26. Smith E, Prasad KM, Butcher M, Dobrian A, Kolls JK, Ley K and Galkina E: Blockade of interleukin-17A results in reduced atherosclerosis in apolipoprotein E-deficient mice. Circulation 121: 1746-1755, 2010.
27. Othumpangat S, Noti JD, McMillen CM and Beezhold DH: ICAM-1 regulates the survival of influenza virus in lung epithelial cells during the early stages of infection. Virology 487: 85-94, 2016.
28. Gabr MA, Jing L, Helbling AR, Sinclair SM, Allen KD, Shamji MF, Richardson WJ, Fitch RD, Setton LA and Chen J: Interleukin-17 synergizes with IFNgamma or TNFalpha to promote inflammatory mediator release and intercellular adhesion molecule-1 (ICAM-1) expression in human intervertebral disc cells. J Orthop Res 29: 1-7, 2011.
29. Plaisance-Bonstaff K and Renne R: Viral miRNAs. Methods Mol Biol 721: 43-66, 2011.
30. Huang J, Zhang SY, Gao YM, Liu YF, Liu YB, Zhao ZG and Yang K: MicroRNAs as oncogenes or tumour suppressors in oesophageal cancer: Potential biomarkers and therapeutic targets. Cell Prolif 47: 277-286, 2014.
31. Li J, You T and Jing J: MiR-125b inhibits cell biological progression of Ewing's sarcoma by suppressing the PI3K/Akt signalling pathway. Cell Prolif 47: 152-160, 2014.
32. Li M, Yu M, Liu C, Zhu H, He X, Peng S and Hua J: miR-34c works downstream of p53 leading to dairy goat male germline stem-cell (mGSCs) apoptosis. Cell Prolif 46: 223-231, 2013.
33. Li Z, Yu X, Shen J and Jiang Y: MicroRNA dysregulation in uveal melanoma: A new player enters the game. Oncotarget 6: 4562-4568, 2015.
34. Xu Z, Asahchop EL, Branton WG, Gelman BB, Power C and Hobman TC: MicroRNAs upregulated during HIV infection target peroxisome biogenesis factors: Implications for virus biology, disease mechanisms and neuropathology. PLoS Pathog 13: e1006360, 2017.
35. Cao Q, Liu F, Ji K, Liu N, He Y, Zhang W and Wang L: MicroRNA-381 inhibits the metastasis of gastric cancer by targeting TMEM16A expression. J Exp Clin Cancer Res 36: 29, 2017.
36. Hou C, Meng F, Zhang Z, Kang Y, Chen W, Huang G, Fu M, Sheng P, Zhang Z and Liao W: The role of MicroRNA-381 in chondrogenesis and interleukin-1-beta induced chondrocyte responses. Cell Physiol Biochem 36: 1753-1766, 2015.
37. Zhang X, Goncalves R and Mosser DM: The isolation and characterization of murine macrophages. Curr Protoc Immunol Chapter 14: Unit 14.1, 2008.
38. Arahata K and Engel AG: Monoclonal antibody analysis of mononuclear cells in myopathies. I: Quantitation of subsets according to diagnosis and sites of accumulation and demonstration and counts of muscle fibers invaded by T cells. Ann Neurol 16: 193-208, 1984.
39. Engel AG and Arahata K: Monoclonal antibody analysis of mononuclear cells in myopathies. II: Phenotypes of autoinvasive cells in polymyositis and inclusion body myositis. Ann Neurol 16: 209-215, 1984.
40. Goebels N, Michaelis D, Engelhardt M, Huber S, Bender A, Pongratz D, Johnson MA, Wekerle H, Tschopp J, Jenne D, *et al*: Differential expression of perforin in muscle-infiltrating T cells in polymyositis and dermatomyositis. J Clin Invest 97: 2905-2910, 1996.
41. Zong M and Lundberg IE: Pathogenesis, classification and treatment of inflammatory myopathies. Nat Rev Rheumatol 7: 297-306, 2011.
42. Notarnicola A, Lapadula G, Natuzzi D, Lundberg IE and Iannone F: Correlation between serum levels of IL-15 and IL-17 in patients with idiopathic inflammatory myopathies. Scand J Rheumatol 44: 224-228, 2015.
43. Yin Y, Li F, Shi J, Li S, Cai J and Jiang Y: MiR-146a regulates inflammatory infiltration by macrophages in polymyositis/dermatomyositis by targeting TRAF6 and affecting IL-17/ICAM-1 pathway. Cell Physiol Biochem 40: 486-498, 2016.
44. Miossec P: Interleukin-17 in fashion, at last: Ten years after its description, its cellular source has been identified. Arthritis Rheum 56: 2111-2115, 2007.
45. Kenna TJ and Brown MA: The role of IL-17-secreting mast cells in inflammatory joint disease. Nat Rev Rheumatol 9: 375-379, 2013.
46. Baeten DL and Kuchroo VK: How Cytokine networks fuel inflammation: Interleukin-17 and a tale of two autoimmune diseases. Nat Med 19: 824-825, 2013.
47. Sallum AM, Kiss MH, Silva CA, Wakamatsu A, Vianna MA, Sachetti S and Marie SK: Difference in adhesion molecule expression (ICAM-1 and VCAM-1) in juvenile and adult dermatomyositis, polymyositis and inclusion body myositis. Autoimmun Rev 5: 93-100, 2006.
48. Szodoray P, Alex P, Knowlton N, Centola M, Dozmorov I, Csipo I, Nagy AT, Constantin T, Ponyi A, Nakken B, *et al*: Idiopathic inflammatory myopathies, signified by distinctive peripheral cytokines, chemokines and the TNF family members B-cell activating factor and a proliferation inducing ligand. Rheumatology (Oxford) 49: 1867-1877, 2010.
49. Tournadre A, Porcherot M, Chérin P, Marie I, Hachulla E and Miossec P: Th1 and Th17 balance in inflammatory myopathies: Interaction with dendritic cells and possible link with response to high-dose immunoglobulins. Cytokine 46: 297-301, 2009.
50. Yin Y, Li F, Shi J, Li S, Cai J and Jiang Y: MiR-146a regulates inflammatory infiltration by macrophages in polymyositis/dermatomyositis by targeting TRAF6 and affecting IL-17/ICAM-1 Pathway. Cell Physiol Biochem 40: 486-498, 2016.
51. Tang Q, Li J, Zhu H, Li P, Zou Z and Xiao Y: Hmgb1-IL-23-IL-17-IL-6-Stat3 axis promotes tumor growth in murine models of melanoma. Mediators Inflamm 2013: 713859, 2013.